

19. White, J. H. *et al.* Heterodimerization is required for the formation of a functional GABA_B receptor. *Nature* **396**, 679–682 (1998).
20. Kaupmann, K. *et al.* GABA_B-receptor subtypes assemble into functional heteromeric complexes. *Nature* **396**, 683–687 (1998).
21. Liu, F. *et al.* Direct protein–protein coupling enables cross-talk between dopamine D₅ and γ -aminobutyric acid A receptors. *Nature* **493**, 274–280 (2000).
22. Dixon, B. S., Sharma, R. V., Dickerson, T. & Fortune, J. Bradykinin and angiotensin II: activation of protein kinase C in arterial smooth muscle. *Am. J. Physiol.* **266**, 406–420 (1994).
23. Tsuchida, S. *et al.* Potent antihypertrophic effect of the bradykinin B₂ receptor system on the renal vasculature. *Kidney Int.* **56**, 509–516 (1999).
24. Bascands, J. L. *et al.* Bradykinin-induced *in vitro* contraction of rat mesangial cells via a B₂ receptor type. *Am. J. Physiol.* **267**, F871–F878 (1994).
25. Zhuo, J. *et al.* Localization and interactions of vasoactive peptide receptors in renomedullary interstitial cells of the kidney. *Kidney Int.* **67**, S22–S28. (1998).
26. Quitterer, U. & Lohse, M. J. Crosstalk between G α_i - and G α_q -coupled receptors is mediated by G $\beta\gamma$ exchange. *Proc. Natl Acad. Sci. USA* **96**, 10626–10631 (1999).
27. Quitterer, U., Zaki, E. & AbdAlla, S. Investigation of the extracellular accessibility of the connecting loop between membrane domains I and II of the bradykinin B₂ receptor. *J. Biol. Chem.* **274**, 14773–14778 (1999).
28. Mastro, R. & Hall, M. Protein delipidation and precipitation by tri-n-butylphosphate, acetone, and methanol treatment for isoelectric focusing and two-dimensional gel electrophoresis. *Anal. Biochem.* **273**, 313–315 (1999).

Supplementary information is available on Nature's World-Wide Web site (<http://nature.com>) or as paper copy from the London editorial office of Nature.

Acknowledgements

We thank B. Nürnberg, for anti-G α -common antibodies, and J. Heukeshoven for helpful advice on high-resolution electrophoresis of hydrophobic proteins. This work was supported in part by the Deutsche Forschungsgemeinschaft.

Correspondence and requests for materials should be addressed to U.Q. (e-mail: toph029@rzbox.uni-wuerzburg.de).

Pilus retraction powers bacterial twitching motility

Alexey J. Merz*†, Magdalene So* & Michael P. Sheetz†‡

*Department of Molecular Microbiology and Immunology, Oregon Health Sciences University, Portland, Oregon 97201-3098, USA

‡Department of Cell Biology, Duke University Medical School, Durham, North Carolina 27705, USA

Twitching and social gliding motility allow many Gram negative bacteria to crawl along surfaces, and are implicated in a wide range of biological functions¹. Type IV pili (Tfp) are required for twitching and social gliding, but the mechanism by which these filaments promote motility has remained enigmatic^{1–4}. Here we use laser tweezers⁵ to show that Tfp forcefully retract. *Neisseria gonorrhoeae* cells that produce Tfp actively crawl on a glass surface and form adherent microcolonies. When laser tweezers are used to place and hold cells near a microcolony, retractile forces pull the cells toward the microcolony. In quantitative experiments, the Tfp of immobilized bacteria bind to latex beads and retract, pulling beads from the tweezers at forces that can exceed 80 pN. Episodes of retraction terminate with release or breakage of the Tfp tether. Both motility and retraction mediated by Tfp occur at about 1 $\mu\text{m s}^{-1}$ and require protein synthesis and function of the PilT protein. Our experiments establish that Tfp filaments retract, generate substantial force and directly mediate cell movement.

Type IV pili are implicated in motility^{1–3,6}, biofilm formation⁷, virulence^{8–11} and all three modes of prokaryotic horizontal genetic transfer (transformation^{12,13}, conjugation¹⁴ and transduction^{15,16}). The Tfp fibre, a helical polymer of the pilin protein, is 6 nm in

diameter and up to several micrometres in length^{17,18}. Type IV pilus biosynthesis occurs through the type II protein translocation pathway and requires several accessory proteins in addition to the pilin subunit¹. The PilT protein is dispensable for Tfp biosynthesis but is essential for both Tfp-mediated motility^{3,19,20} and for the DNA uptake step of genetic transformation^{13,20}. PilT belongs to a highly conserved family of presumed ATPases, which partition to the inner membrane and cytosol and are thought to energize type II and IV protein translocation systems^{1,4,19,21}. Two proteins of this family form hexameric rings strikingly similar to the rings formed by many AAA-type ATP-dependent chaperones and proteases²². Electron-microscope studies of *pilT* mutants led to the hypothesis that Tfp promote cellular motility by retracting^{3,15}, perhaps through PilT-mediated filament disassembly^{1,4,19}. Indirect evidence further suggests that other bacterial surface filaments might retract, including the conjugative F pili of *Escherichia coli*²³ and a type III export filament of *Salmonella enteritidis* associated with cell contact²⁴. However, filament retraction has been neither observed directly nor proven to power motility in any prokaryotic system.

N. gonorrhoeae, the causative agent of gonorrhoea, provides an excellent model for studies of twitching motility. It lacks rotary flagella and components for type III export, and it produces only one known fimbrial structure, the Tfp. When we suspended Tfp-producing *N. gonorrhoeae* cells at low density in liquid medium, they attached to and crawled over the surface of a glass coverslip (Fig. 1). Under optimal conditions (see Methods), over half of the bacteria on the coverslip were motile. Figure 1b depicts the path of a crawling diplococcus (a joined pair of cells is the neisserial functional unit). Although most movements were short and directional changes occurred frequently, many directed movements of 2–5 μm were observed. Cells crawled at $\sim 1 \mu\text{m s}^{-1}$ (Fig. 1c, d). This motility was not due to passive diffusion. Motile cells consistently crawled

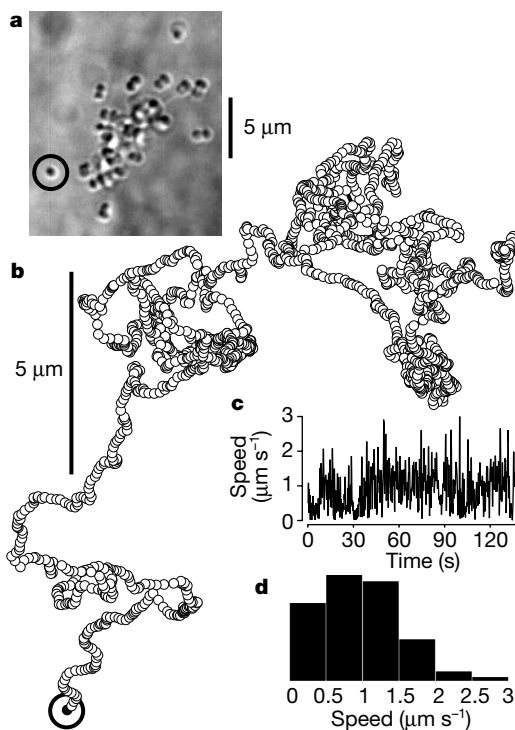


Figure 1 Piliated *N. gonorrhoeae* cells crawl on an inert surface. **a**, Cells crawling on a glass coverslip. This is the first frame of the sequence analysed in **b–d**, and the tracked diplococcus is circled. Note that most cells are present as diplococci. **b**, Tracking of the diplococcus indicated in **a** during an interval of 140 s. Small circles show the position of the tracked diplococcus at intervals of 67 ms. Large circle indicates the start point. **c**, Plot of velocity against time for the same track. **d**, Histogram of the velocities shown in **c**.

† Present addresses: Department of Biochemistry, Dartmouth Medical School, Hanover, New Hampshire 03755-3844, USA (A.J.M.); Department of Biological Sciences, Columbia University, New York, New York 10027, USA (M.P.S).

out of a laser-tweezers trap strong enough to firmly arrest suspended cells or 1- μm latex beads (20 pN at 100 nm displacement). Cells crawled at temperatures from 20 to 42 °C. Motility ceased ~ 10 min after the addition of chloramphenicol or tetracycline and resumed upon drug washout, indicating a requirement for protein synthesis (Table 1). Similarly, bacteria were non-motile and unable to grow in defined medium lacking L-glutamine and pyruvate, and became motile upon addition of these nutrients. As expected, non-piliated *pilE* and *pilF* mutants were completely non-motile. Three piliated *pilT* mutants also failed to undergo large movements ($> 1 \mu\text{m}$) and never crawled out of the laser trap (Table 1). *N. gonorrhoeae* cells thus can crawl over surfaces at rates of $\sim 1 \mu\text{m s}^{-1}$ by an active process requiring protein synthesis, Tfp biogenesis and PilT^{3,19,20}.

Tfp-producing *N. gonorrhoeae* cells not only crawl but aggregate into microcolonies that contain twitching or writhing cells. Cells within 1–5 μm of a microcolony often move into the colony, whereas cells within a microcolony move out of the colony^{2,6–8}. To determine whether retractile forces would pull dispersed cells together, we used laser tweezers to position isolated cells 1–5 μm (1–2 pilus lengths) away from microcolonies attached to a coverslip (Fig. 2). The trapped cells were repeatedly pulled from the laser trap toward the microcolonies, directly showing that there are retractile forces between cells (Fig. 2a). The cells were pulled towards the microcolonies at speeds of $\sim 1 \mu\text{m s}^{-1}$, the same rate at which cells crawled on coverslips (Figs 1 and 2a). Cells pulled from the laser trap sometimes bound irreversibly to the microcolonies, but more often were released back into the laser trap (Fig. 2a). Upon release, the tethers between cells were broken, as trapped cells could be moved freely away from the microcolony using the laser tweezers. When released cells were moved $\sim 10 \mu\text{m}$ away and then placed near the opposite side of the same microcolony, they were again pulled out of the trap toward the microcolony (Fig. 2b). Retraction and tethering are therefore transient and can be re-established. In contrast, when we carried out identical manipulations using piliated, non-motile *pilT* mutants, cells were never pulled from the trap (Table 1), although nonretractile static tethers between the trapped cells and the microcolonies sometimes formed (data not shown). Together these experiments show that episodes of PilT-dependent Tfp retraction pull bacterial cells towards one another over distances of up to 5 μm at speeds of $\sim 1 \mu\text{m s}^{-1}$.

Quantitative analyses of Tfp retraction are impeded by variations in cell morphology and by experimental geometries in which two groups of cells pull toward one another. We therefore developed a bead-based assay for Tfp retraction (Fig. 3a). Individual diplococci were immobilized on 3- μm latex beads that had first been coated with anti-*N. gonorrhoeae* antiserum and anchored to the coverslip. Smaller 1- μm beads, coated with a monoclonal antibody that recognizes a surface-exposed epitope on the Tfp fibre, were introduced into the sample chamber. Laser tweezers were then used to hold the 1- μm beads near the immobilized diplococci so that the beads could interact with Tfp.

When anti-pilus 1- μm beads were placed within 1–3 μm of immobilized cells, the beads became dynamically tethered and were repeatedly pulled towards the immobilized cells (Fig. 3b). The mean speed of retraction was $1.17 \pm 0.49 \mu\text{m s}^{-1}$ (mean \pm s.d.; $n = 713$), and was independent of the distance traversed by the beads (Fig. 3c). Retraction events were separated by intervals of 1–20 s. One-micrometre beads lacking the anti-pilin monoclonal antibody did not bind to pili as frequently as anti-pilin beads; but when they bound, they also were pulled toward immobilized bacteria. Type IV pili therefore exert retractile force through both nonspecific and specific binding interactions, consistent with our finding that Tfp facilitate bacterial motility on inert substrates (Fig. 1). Retraction ceased ~ 10 min after the addition of chloramphenicol or tetracycline and resumed after drug washout, again indicating a requirement for protein synthesis.

The restoring force of the laser tweezers increases with radial displacement from the trap centre, and can be calibrated for homogeneous particles using laminar flow (see Methods). Figure 3c shows a trace of displacement against time, with force shown on the displacement axis. Isolated, immobilized diplococci were often able to exert forces of 80 pN or more on trapped 1- μm beads. By comparison, ~ 20 pN is the force needed to extract an integral membrane protein from a lipid bilayer²⁵, and ~ 30 pN of tensile force is sufficient to elongate a microvillus on a host cell²⁶.

Retraction usually terminated with release or breakage of the pilus tether and bead movement back into the laser trap (Fig. 3b, c). Transitions from retraction to release usually occurred in less than 67 ms. The velocities of bead movement back into the trap (Fig. 3c) were much more variable than retraction speeds and were proportional to the distance displaced before release ($4.34 \pm 3.48 \mu\text{m s}^{-1}$;

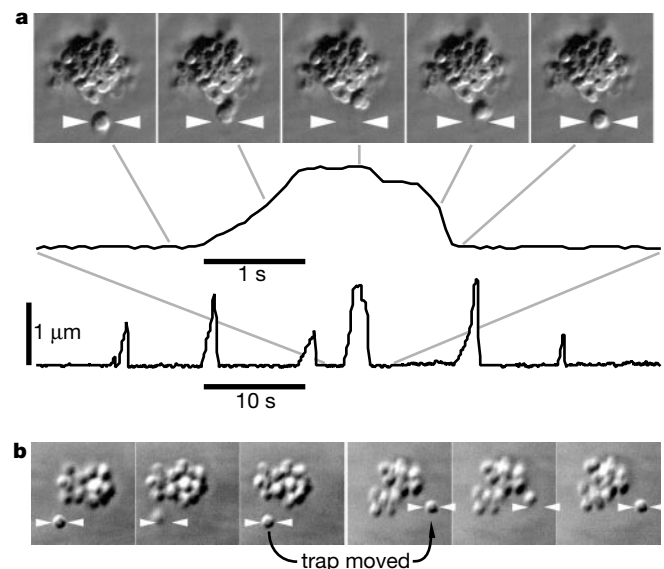


Figure 2 Optical tweezers reveal retractile forces between piliated *N. gonorrhoeae* cells. **a**, Cell–microcolony assay. A diplococcus held in the laser-tweezers trap (indicated by arrowheads) was repeatedly pulled toward a microcolony attached to the coverslip. Micrographs (separated by ~ 1 -s intervals) show one retraction event from the sequence used to generate the trace. Traces indicate radial displacement of the trapped diplococcus from the centre of the laser trap. The top trace shows a time-magnified portion of the bottom trace. Note that retraction occurs at $\sim 1 \mu\text{m s}^{-1}$. **b**, Retraction and tethering are transient and can be re-established. A diplococcus was trapped and positioned next to a microcolony as in **a**. The diplococcus was pulled from the trap towards the microcolony and then released back into the trap (first three panels). Next, the trap and trapped diplococcus were moved more than 10 μm away from the microcolony, then repositioned on the opposite side of the same microcolony, where the diplococcus was again pulled from the trap towards the microcolony (last three panels).

Table 1 Motility and retraction phenotypes of *N. gonorrhoeae* strains

	Crawling	Cell–cell retraction	Cell–bead retraction
MS11 N400	Yes	Yes	n.d.
MS11 GT102 <i>pilT</i> _{ΔO₂L}	No	No	n.d.
MS11 GT103 <i>pilT</i> ::mTnEGNS	No	No	n.d.
MS11 AM92	Yes	Yes	Yes
MS11 AM92T1 <i>pilT</i> ::mTnEGNS	No	No	No
MS11 AM92			
+ Tetracycline	No	n.d.	No
+ Chloramphenicol	No	n.d.	No
–L-glutamine and pyruvate	No	n.d.	n.d.
20 °C (cell-division block)	Yes	n.d.	Yes

n.d., not determined.

$n = 171$). Release events could result from force-regulated release of the fibre at a threshold tension level, from breakage of the retracting fibre or the basal body, or from dissociation of the retracting fibre from the 1- μm bead. More detailed analyses of many traces made at laser power levels of 400 and 800 mW (Fig. 3e) indicated that bead release is dependent on force, and is not solely a function of linear displacement. Histograms of the forces reached before bead release show small peaks at about 40, 60 and 90 pN (Fig. 3e, arrows). Studies of other motor-dependent movements have also revealed peaks in displacement histograms. These peaks have been interpreted as multiples of the critical force generated by the motors²⁷. The peaks observed in our study may reflect the presence of multiple retracting fibres or multiple motor units on a single fibre; however, we stress that additional, more refined measurements will be required to establish the unit critical force of the Tfp retraction machinery.

As in the cell–microcolony assays, *pilT* mutant cells were unable to generate retractile forces but could sometimes form static tethers to laser-trapped 1- μm beads. When a tethered bead was held in a stationary laser-tweezers trap, movement of the microscope stage

(and hence the immobilized bacterium) within a defined radius did not displace the tethered 1- μm bead out of the trap, but movement outside this radius displaced the tethered bead from the trap centre (Fig. 3f). The static character of the tether was tested by placing the tethered bead under tension, 0.2 μm from the centre of the trap. No further displacements of the bead (> 25 nm) occurred over a period of more than 120 s, indicating that the tether was static (Fig. 3f). These results confirm that PilT is essential for Tfp retraction.

What is the mechanism of Tfp retraction? The available evidence is most consistent with molecular ratchet models²⁸ in which retractile force is generated by filament disassembly into the inner membrane. Genetic analyses suggest that PilT promotes pilin disassembly, pilin degradation, or both^{4,19}. PilT, like the closely related ATPases thought to energize Tfp assembly and type II and IV secretion, localizes to the cytoplasm and inner membrane^{1,13,19,21}. Unassembled pilin is a type II integral inner membrane protein²⁹. Upon assembly, the membrane-spanning domain of pilin moves into a hydrophobic coiled-coil at the core of the polymeric fibre^{17,18}. These observations support models in which cytoplasmic ATPases

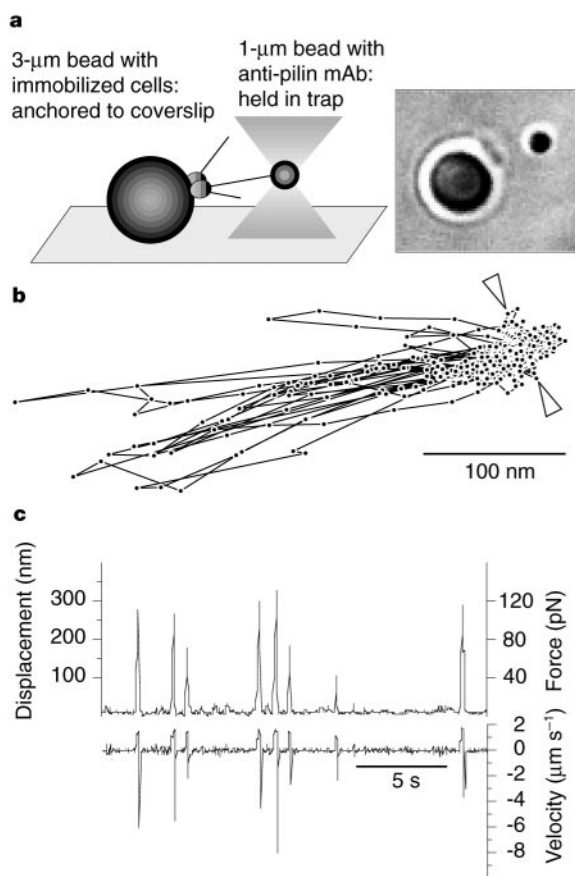
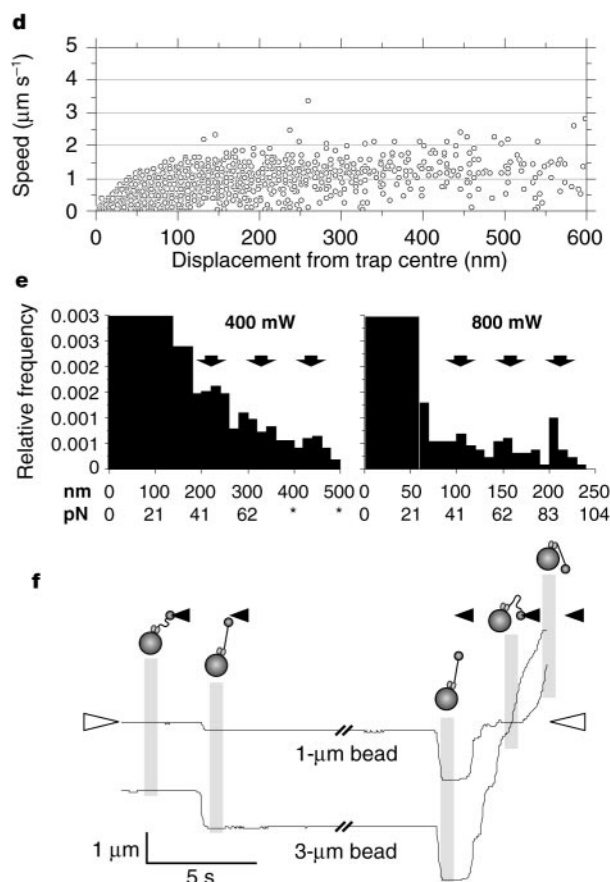


Figure 3 Quantitative type IV pili retraction assay. **a**, Experimental geometry. The cartoon shows a side view; the micrograph shows the assay in progress from above, with scale indicated by the beads (1 and 3 μm). **b**, Direction of displacements. Trace from a recording of a single immobilized diplococcus that shows the locations of the 1- μm bead centroid in the plane parallel to the coverslip surface. The centre of the laser trap is indicated (arrowheads). The immobilized diplococcus is in the same position relative to the laser trap as in the micrograph in **a**. **c**, Velocity, timing and force of retraction. Top trace, radial displacement of the 1- μm bead versus time, and calibrated restoring force imposed by the laser-tweezers trap. Bottom trace, velocities of retraction and release from the same recording. Positive velocities denote displacement away from the trap centre (toward the immobilized cells), and negative velocities denote release into the trap centre **d**, Plot of retraction velocity versus displacement, showing pooled data from recordings of



14 different immobilized diplococci. Note that for displacements of 100 nm or more, retraction velocities are relatively constant at $\sim 1 \mu\text{m s}^{-1}$. **e**, Histograms of forces reached prior to bead release at 400 and 800 mW input laser power. **f**, Static tethering of 1- μm beads by immobilized *pilT* mutant cells. Cartoons show interpretation of the traces. The Tfp could not be seen, but their state (slack or under tension) was inferred from movements of the 1- μm bead relative to the trap. Arrowheads denote the position of the laser trap (filled for the cartoons, open for the trace), which was stationary throughout the experiment. The 3- μm bead was attached to the coverslip on the microscope stage, and was moved using a stage motor. Traces show the displacements of the 1- μm and 3- μm beads relative to the laser trap plotted against time. Breaks in the traces denote an interval of more than 120 s in which there were no movements more than 25 nm of the 1- μm bead.

catalyse pilus extension and retraction from the base of the pilus fibre, within the plane of the inner membrane. The Tfp filament is a single-stranded helix with five pilin subunits per turn and a 40 Å pitch^{17,18}. Assembly and disassembly are therefore predicted to occur in 8 Å steps, consistent with the high levels of retractile force observed (Figs. 3c, e). Retraction mediated by disassembly at the observed rate of 1.2 μm s⁻¹ (Fig. 3d) would entail the removal of 1,500 pilin subunits per second from the fibre base.

Pilus retraction is thought to occur in several bacterial systems^{3,4,15,19,23,24}. To our knowledge our experiments provide the first direct observations of pilus retraction and may provide a model for understanding related retractile processes. In *N. gonorrhoeae*, DNA transformation facilitates pilin antigenic variation¹² and other horizontal genetic transfer functions. Like twitching motility, DNA uptake requires Tfp biosynthesis and PilT function^{13,20}. Moreover, many bacteria use PilT or PilT orthologues for DNA uptake, including species that lack Tfp. Consistent with the hypothesis that DNA uptake and pilus retraction use a common machinery, the rate of processive DNA uptake in *Haemophilus influenzae* (~0.17 μm s⁻¹; ref. 13) is comparable to the speed of Tfp retraction in our experiments. A broadly conserved mechanism may therefore power not only pilus retraction, but also other macromolecular translocation processes. Finally, PilT and twitching motility are implicated in virulence-related functions^{8–10}. Eukaryotic cells sense and respond to mechanical forces³⁰, and *N. gonorrhoeae* Tfp and PilT function together to elicit adhesive plaque formation in epithelial cells¹¹; we therefore propose that the mechanical forces generated by retractile pili are important and previously overlooked signals between pathogenic bacteria and host cells. □

Methods

Bacterial strains and media

N. gonorrhoeae were maintained on GCB agar with supplements (Difco). Antibiotics (Sigma) were used at the following concentrations (in mg l⁻¹): kanamycin, 100; erythromycin, 4; tetracycline, 50; chloramphenicol, 40. We carried out motility assays in phenol red-free DMEM (Gibco BRL), supplemented with L-glutamine, pyruvate and 1% (w/v) bovine serum albumin (BSA) fraction V (Sigma). BSA limited the adsorption of bacteria onto the glass coverslips and was essential for optimal motility. MS11 N400 and its isogenic derivatives GT102 (*pilTΔQSL*) and GT103 (*pilT::mTnEGNS*) were gifts from M. Koomey²⁰. MS11 AM92 is an MS11A derivative that produces a pilin variant recognized by monoclonal antibody 20D910 (ref. 10). The *pilT::mTnEGNS* allele from GT103 was moved into MS11 AM92 by DNA transformation, then backcrossed against MS11 AM92 three times to generate AM92T1. AM92 and AM92T1 are pilated as judged by immunofluorescent staining with monoclonal antibody 20D9 and by immunoblotting with monoclonal antibodies 20D9 and 10H5 (anti-SM1 epitope). As expected, AM92 is pilated, motile, competent for DNA transformation, and elicits cortical plaques in epithelial cells, whereas AM92T1 is pilated, non-motile, transformation deficient and exhibits defective cortical plaque induction^{11,12,20}.

Bead-based retraction assay

Three-micrometre latex beads (Bangs Laboratories) were coated with rabbit anti-*N. gonorrhoeae* antiserum by passive adsorption as recommended by the supplier. The beads were washed thoroughly in PBS (phosphate-buffered saline, pH 7.4) and adsorbed onto clean coverslips in the presence of PBS. Coverslips were washed in PBS to remove unbound beads and blocked in DMEM with 1% BSA at 25°C for 15 min or more before use. One-micrometre beads were coated with biotinylated monoclonal antibody 20D9 by a sandwich method³⁰. One-micrometre beads (Polysciences) were covalently coupled to biotinylated casein (Sigma). Biotinylated monoclonal antibody 20D9 (prepared with sulpho-NHS biotin; Pierce) was then linked to the biotinylated casein by an avidin bridge; control beads lacked monoclonal antibody 20D9. The beads were blocked with biotinylated BSA (biotinamido caproyl BSA; Sigma) and washed thoroughly. A dot blot assay indicated that roughly 5 × 10³ molecules of monoclonal antibody 20D9 bound per bead. A serial perfusion method greatly reduced aggregate formation among the beads and cells. Coverslips with attached 3-μm beads were used to form the bottom surface of a perfusion chamber, which was placed on the microscope stage. A dilute, vortex-dispersed suspension of *N. gonorrhoeae* cells in DMEM with 1% BSA was perfused into the chamber. We monitored bacterial binding to the anchored 3-μm beads by microscope. When 10–20% of the 3-μm beads had bound 1 or 2 diplococci, unbound bacteria were washed out. One-micrometre beads were suspended in DMEM with 1% BSA and dispersed by bath sonication, then perfused into the sample chamber and manipulated using the laser tweezers. Except where indicated, we carried out assays at 35°C.

Laser trapping and single particle tracking

The optical tweezers workstation was configured as described⁵ and included a Zeiss Axiocvert microscope, a Nd-YAG laser (1,064-nm wavelength) directed into the bottom port of the microscope, a piezoelectric stage controller, and a Nuvicon camera with analogue signal processor and S-VHS video recorder for data capture. We carried out video digitization and data analysis on a SGI workstation running Isee particle tracking software (Inovision). Speeds of crawling bacteria (Fig. 1c, d) were obtained by calculating centroid position using a moving average function with a three-frame window to minimize artefacts arising from the irregular shapes of the cells. In the bead-based assay, velocities were calculated frame by frame. Positive velocities were assigned to displacements away from the trap centre (retraction) and negative velocities were assigned to movement toward the trap centre (release). Values less than three times the r.m.s. retraction or release velocities were discarded as noise. The remaining values were used to calculate the mean retraction and release velocities shown in the text. Results obtained by this method agreed with results obtained by hand-fitting the slopes of displacement versus time plots for individual retraction events. The trap force calibration was done as described⁵.

Received 28 April; accepted 20 June 2000.

- Wall, D. & Kaiser, D. Type IV pili and cell motility. *Mol. Microbiol.* **32**, 1–10 (1999).
- Henrichsen, J. Twitching motility. *Annu. Rev. Microbiol.* **37**, 81–93 (1983).
- Bradley, D. E. A function of *Pseudomonas aeruginosa* PAO polar pili: twitching motility. *Can. J. Microbiol.* **26**, 146–154 (1980).
- Wolfgang, M., Park, H. S., Hayes, S. E., van Putten, J. P. M. & Koomey, M. Switching of an absolute defect in type IV pilus biogenesis by loss-of-function mutations in *pilT*, a twitching motility gene in *Neisseria gonorrhoeae*. *Proc. Natl Acad. Sci. USA* **95**, 14973–14978 (1998).
- Sheetz, M. P. (ed.) *Laser Tweezers in Cell Biology* (Academic, New York, 1997).
- Swanson, J. Studies on gonococcus infection. XII. Colony color and opacity variants of gonococci. *Infect. Immun.* **19**, 320–331 (1978).
- O'Toole, G. A. & Kolter, R. Flagellar and twitching motility are necessary for *Pseudomonas aeruginosa* biofilm development. *Mol. Microbiol.* **30**, 295–304 (1998).
- Bieber, D. et al. Type IV pili, transient bacterial aggregates, and virulence of enteropathogenic *Escherichia coli*. *Science* **280**, 2114–2118 (1998).
- Comolli, J. C. et al. *Pseudomonas aeruginosa* gene products PilT and PilU are required for cytotoxicity in vitro and virulence in a mouse model of acute pneumonia. *Infect. Immun.* **67**, 3625–3630 (1999).
- Pujol, C., Eugene, E., Marceau, M. & Nassif, X. The meningococcal PilT protein is required for induction of intimate attachment to epithelial cells following pilus-mediated adhesion. *Proc. Natl Acad. Sci. USA* **96**, 4017–4022 (1999).
- Merz, A. J., Enns, C. A. & So, M. Type IV pili of pathogenic *Neisseriae* elicit cortical plaque formation in epithelial cells. *Mol. Microbiol.* **32**, 1316–1332 (1999).
- Seifert, H. S., Ajioka, R. S., Marchal, C., Sparling, P. F. & So, M. DNA transformation leads to pilin antigenic variation in *Neisseria gonorrhoeae*. *Nature* **336**, 392–395 (1988).
- Dubnau, D. DNA uptake in bacteria. *Annu. Rev. Microbiol.* **53**, 217–244 (1999).
- Yoshida, T., Kim, S. R. & Komano, T. Twelve *pil* genes are required for biogenesis of the R64 thin pilus. *J. Bacteriol.* **181**, 2038–2043 (1999).
- Bradley, D. E. Evidence for the retraction of *Pseudomonas aeruginosa* RNA phage pili. *Biochem. Biophys. Res. Commun.* **47**, 142–149 (1972).
- Karaolis, D. K., Somara, S., Maneval, D. R. Jr, Johnson, J. A. & Kaper, J. B. A bacteriophage encoding a pathogenicity island, a type-IV pilus and a phage receptor in cholera bacteria. *Nature* **399**, 375–379 (1999).
- Parge, H. E. et al. Structure of the fibre-forming protein pilin at 2.6 Å resolution. *Nature* **378**, 32–38 (1995).
- Forest, K. T. & Tainer, J. A. Type-4 pilus structure: outside to inside and top to bottom—a minireview. *Gene* **192**, 165–169 (1997).
- Whitchurch, C. B., Hobbs, M., Livingston, S. P., Krishnapillai, V. & Mattick, J. S. Characterisation of a *Pseudomonas aeruginosa* twitching motility gene and evidence for a specialised protein export system widespread in eubacteria. *Gene* **101**, 33–44 (1991).
- Wolfgang, M. et al. *pilT* mutations lead to simultaneous defects in competence for natural transformation and twitching motility in pilated *Neisseria gonorrhoeae*. *Mol. Microbiol.* **29**, 321–330 (1998).
- Brossay, L., Paradis, G., Fox, R., Koomey, M. & Hebert, J. Identification, localization, and distribution of the PilT protein in *Neisseria gonorrhoeae*. *Infect. Immun.* **62**, 2302–2308 (1994).
- Krause, S. et al. Sequence-related protein export NTPases encoded by the conjugative transfer region of RP4 and by the *cag* pathogenicity island of *Helicobacter pylori* share similar hexameric ring structures. *Proc. Natl Acad. Sci. USA* **97**, 3067–3072 (2000).
- Novotny, C. P. & Fives-Taylor, P. Retraction of F pili. *J. Bacteriol.* **117**, 1306–1311 (1974).
- Ginocchio, C. C., Olmsted, S. B., Wells, C. L. & Galan, J. E. Contact with epithelial cells induces the formation of surface appendages on *Salmonella typhimurium*. *Cell* **76**, 717–724 (1994).
- Evans, E., Berk, D. & Leung, A. Detachment of agglutinin-bonded red blood cells. I. Forces to rupture molecular-point attachments. *Biophys. J.* **59**, 838–848 (1991).
- Shao, J. Y., Ting-Beall, H. P. & Hochmuth, R. M. Static and dynamic lengths of neutrophil microvilli. *Proc. Natl Acad. Sci. USA* **95**, 6797–6802 (1998).
- Coppin, C. M., Finer, J. T., Spudich, J. A. & Vale, R. D. Detection of sub-8-nm movements of kinesin by high-resolution optical-trap microscopy. *Proc. Natl Acad. Sci. USA* **93**, 1913–1917 (1996).
- Mahadevan, L. & Matsudaira, P. Motility powered by supramolecular springs and ratchets. *Science* **288**, 95–100 (2000).
- Dupuy, B., Taha, M. K., Pugsley, A. P. & Marchal, C. *Neisseria gonorrhoeae* prepilin export studied in *Escherichia coli*. *J. Bacteriol.* **173**, 7589–7598 (1991).
- Felsenfeld, D. P., Schwartzberg, P. L., Venegas, A., Tse, R. & Sheetz, M. P. Selective regulation of integrin-cytoskeleton interactions by the tyrosine kinase Src. *Nature Cell Biol.* **1**, 200–206 (1999).

Acknowledgements

We thank our colleagues in the Sheetz and So labs for invaluable technical assistance and

stimulating discussions; E. Barklis and L. Kenney for critical comments on the manuscript; and M. Koomey for providing bacterial strains. This work was supported by NIH grants to M.S. and M.P.S. A.J.M. received pre-doctoral support from an NIH NRSA grant and postdoctoral support from the Cancer Research Fund of the Damon Runyan-Walter Winchell Foundation.

Correspondence and requests for materials should be addressed to M.P.S. (e-mail: ms2001@columbia.edu).

TFIIH is negatively regulated by cdk8-containing mediator complexes

Sasha Akoulitchev, Sergei Chuikov & Danny Reinberg*

Howard Hughes Medical Institute, Division of Nucleic Acids Enzymology, Department of Biochemistry, Robert Wood Johnson Medical School, Piscataway, New Jersey 08854, USA

The mammalian cyclin-dependent kinase 8 (cdk8)¹ gene has been linked with a subset of acute lymphoblastic leukaemias², and its corresponding protein has been functionally implicated in regulation of transcription^{3,4}. Mammalian cdk8 and cyclin C, and their respective yeast homologues, Srb10 and Srb11, are components of the RNA polymerase II holoenzyme complex^{5,6} where they function as a protein kinase that phosphorylates the carboxy-terminal domain (CTD) of the largest subunit of RNA polymerase II (ref. 7). The yeast *SRB10* and *SRB11* genes have been implicated in the negative regulation of transcription⁸. The cdk8/cyclin C protein complex is also found in a number of mammalian Mediator-like protein complexes^{3,5,9–12}, which repress activated transcription independently of the CTD *in vitro*^{9,10}. Here we show that cdk8/cyclin C can regulate transcription by targeting the cdk7/cyclin H subunits of the general transcription initiation factor IIH (TFIIH). cdk8 phosphorylates mammalian cyclin H in the vicinity of its functionally unique amino-terminal and carboxy-terminal α -helical domains¹³. This phosphorylation represses both the ability of TFIIH to activate transcription and its CTD kinase activity. In addition, mimicking cdk8 phosphorylation of cyclin H *in vivo* has a dominant-negative effect on cell growth. Our results link the Mediator complex and the basal transcription machinery by a regulatory pathway involving two cyclin-dependent kinases. This pathway appears to be unique to higher organisms.

The stimulation of gene-specific transcription by transcriptional activator proteins requires coactivators—molecules that mediate communication between the general transcription machinery and the activators. Some transcription coactivators are activator- or gene-specific, whereas others are required for more global gene transcription (general coactivators). General coactivators include PC4, TFIIA and components of the TFIID and RNA polymerase II (RNAPII) holoenzyme complexes. Coactivators in the RNAPII holoenzyme appear to be modular in nature, forming distinct subcomplexes that are capable of positively or negatively regulating transcription¹². Distinct coactivator complexes have been isolated from mammalian cells. One such complex is NAT⁹, which appears to be functionally similar to the mammalian SMCC–TRAP complex¹⁰ and which contains subsets of polypeptides present in other mammalian coactivator complexes such as Mediator¹¹, DRIP¹⁴, CRSP¹⁵ and ARC¹⁶. A unique feature of NAT, Mediator and SMCC–TRAP complexes is the presence of cdk8 and cyclin C, which are the human homologues of yeast Srb10 and Srb11, respectively. The Srb10/11 complex and the NAT complex down-regulate transcription by phosphorylating the CTD of RNAPII before its association with transcription initiation complexes^{7,9};

however, NAT also downregulates transcription independently of the CTD of RNAPII⁹. Notably, other cdk8-containing complexes, such as SMCC–TRAP and Mediator, can function as coactivators of transcription when the reconstituted system is supplemented with a crude protein fraction¹¹ or when the system is reconstituted with PC4 in the absence (or with limiting amounts) of TFIIH¹⁰.

To investigate further the mechanism by which cdk8 negatively regulates transcription, we isolated the NAT and SMCC–TRAP complexes^{9,10}, and analysed their effects on transcription as a function of TFIIH (Fig. 1a). In the absence of TFIIH, both complexes enhanced VP16-mediated activation of transcription. However, both complexes mediated the repression of activated transcription in the TFIIH-dependent assay. Notably, a NAT complex containing a kinase-deficient mutant of cdk8 (D173A) did not support repression (Fig. 1b–d). Treatment of immunoadsorbed, highly purified TFIIH with recombinant cdk8/cyclin C under kinase conditions impaired transcription in a phosphatase-reversible manner (Fig. 1e), which indicates that the cdk8 kinase can downregulate transcription by phosphorylating TFIIH.

The transcription system described above requires PC4, which is downregulated by phosphorylation¹⁷, and it has been suggested that cdk8 targets PC4 (ref. 10). To deduce the *in vivo* target of cdk8, we reconstituted activated transcription in the absence of PC4 using a coactivator complex devoid of cdk8; cdk8 was added exogenously to the assays. We purified and analysed Mediator-like complexes that were devoid of cdk8 but contained polypeptides found in other coactivator complexes (see Supplementary Information). The Mediator-like complex displayed properties similar to those

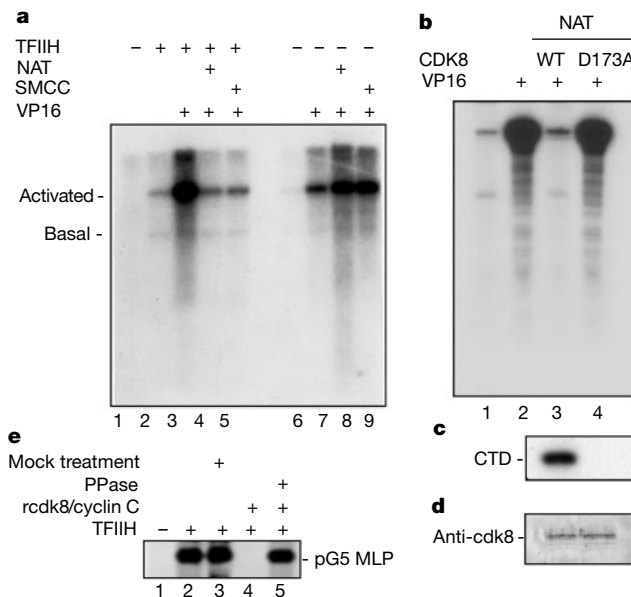


Figure 1 TFIIH mediates cdk8-dependent repression by NAT. **a**, TFIIH-dependent activities of NAT and SMCC complexes. NAT and SMCC–TRAP complexes were purified as described^{9,10}, and their activities analysed using a reconstituted VP16-dependent transcription activation assay in the presence of PC4. Linear (lanes 1–5) or supercoiled (lanes 6–9) DNA templates were used in the assays, and transcription activity was measured in the presence and absence of TFIIH, respectively. The supercoiled template was used to render the assay independent of TFIIH²⁹. The positions of the activated and basal transcription products are indicated. **b–d**, Repression by NAT is cdk8 dependent. NAT was immunoprecipitated from 293T cells expressing wild-type cdk8 (WT) or the kinase-deficient mutant³ of cdk8 (D173A). The preparation was assayed by TFIIH-dependent activated transcription (**b**), CTD kinase assay (**c**) and western blot (**d**). **e**, Cdk8 phosphorylates and inactivates TFIIH. PPase, alkaline phosphatase.